

A Solid-State Supramolecular Rotator Assembled from a Cs-crown Ether Polyoxometalate Hybrid: $(\text{Cs}^+)_3([\text{18}]\text{crown-6})_3(\text{H}^+)_2[\text{PMo}_{12}\text{O}_{40}]$

Tomoyuki Akutagawa,^{*,†,‡,§} Daigoro Endo,[‡] Fumito Kudo,[‡] Shin-ichiro Noro,^{†,‡}
Sadamu Takeda,[△] Leroy Cronin,[⊥] and Takayoshi Nakamura^{*,†,‡,§}

Research Institute for Electronic Science, Hokkaido University, Sapporo 060-0812, Japan, Graduate School of Environmental Earth Science, Hokkaido University, Sapporo 060-0810, Japan, CREST, Japan Science and Technology Agency (JST), Kawaguchi 332-0012, Japan, Graduate School of Science, Hokkaido University, Sapporo 060-0810, Japan, and WestCHEM, Department of Chemistry, University of Glasgow, Glasgow G12 8QQ, U.K.

Received December 26, 2006; Revised Manuscript Received October 17, 2007

ABSTRACT: A solid-state molecular rotator comprising [18]crown-6 was assembled into a crystalline array of $(\text{Cs}^+)_3([\text{18}]\text{crown-6})_3(\text{H}^+)_2[\text{PMo}_{12}\text{O}_{40}]^{5-}$, whereby two $\text{Cs}^+([\text{18}]\text{crown-6})$ supramolecular rotators were complexed with a two-electron-reduced $\alpha\text{-}[\text{PMo}_{12}\text{O}_{40}]^{5-}$ Keggin cluster. The size-compatible rotators of [18]crown-6 were directly complexed to an $\alpha\text{-}[\text{PMo}_{12}\text{O}_{40}]^{5-}$ axle through $\text{Cs}^+\text{-O}$ interactions. The investigation of the dynamics of the system revealed that two rotation frequencies for [18]crown-6 were observed by using temperature-dependent ^1H NMR studies, and these were dominated by intermolecular interactions in the solid state.

Artificial molecular rotors have been extensively investigated as components of nanoscale molecular machines.¹ For example, the design of triptycene, catenane, and rotaxane derivatives that undergo unidirectional molecular rotation is driven by a photothermal isomerization process that has been successfully achieved in solution.² Despite this progress, the assembly of molecular motors capable of unidirectional molecular rotation in the solid state and capable of doing work has not been realized. The design of such systems is a significant challenge because of the competition between packing forces and the need to incorporate a rotator and stator that is free to rotate about a fixed axis. Despite these limitations, there are several examples of systems that are getting closer to these goals. In these systems, a design principle based upon cage-type molecules, such as molecular gyroscopes, turnstiles, and so forth, is used.^{3–5}

In our approach to this challenging problem, we have recently developed a supramolecular cation system, which is constructed from the complexation of crown-ether metal ion complexes, M^+ ([18]crown-6), as counter cations of $[\text{Ni}(\text{dmit})_2]^-$ ($\text{dmit}^{2-} = 2\text{-thione-1,3-dithiole-4,5-dithiolate}$) anions.^{6,7} The idea behind the use of the planar π -delocalized $[\text{Ni}(\text{dmit})_2]$ building-block is to attempt to introduce a magnetic and conducting moiety into the solid-state molecular rotator system.⁶ For example, the thermally activated rotation of [18]crown-6 with a rotational frequency of ~ 60 kHz at ~ 300 K has been confirmed in $(\text{Cs}^+)_2([\text{18}]\text{crown-6})_3[\text{Ni}(\text{dmit})_2]^{2-}$, in which the rotation of [18]crown-6 was coupled with the magnetic properties through distortions in the $[\text{Ni}(\text{dmit})_2]^-$ sublattice at ~ 220 K.^{7a} In addition, a route to biasing the molecular rotation was achieved by applying hydrostatic pressure to the crystals, which could be monitored from the changes in the temperature-dependent magnetic susceptibilities.^{7a} Another solid-state rotator system comprised of anilinium and adamantylammonium complexed on [18]crown-6 has been developed in the complex (anilinium)([18]crown-

6) $[\text{Ni}(\text{dmit})_2]^-$ and (adamantylammonium)([18]crown-6) $[\text{Ni}(\text{dmit})_2]^-$ salts; here, two kinds of rotation frequencies were observed in the solid state.^{7c,d}

Here, we report the extension of our approach by replacing the $[\text{Ni}(\text{dmit})_2]$ unit with a Keggin-type polyoxometalate (POM) cluster, $[\text{PMo}_{12}\text{O}_{40}]$, because it has potential as a redox-active anion species and as a nanoscale space unit.^{8–10} The planar π -conjugated $[\text{Ni}(\text{dmit})_2]$ complex exhibits rich magnetic and electrical conducting properties according to the oxidation states of the complex, whereas the $[\text{PMo}_{12}\text{O}_{40}]$ Keggin ion has variable redox and protonation states, making it potentially useful in catalysis and as a switchable electronic unit for nanoscale materials.⁹ A strong coupling between the molecular motion within our rotor-guest system and the magnetic properties of $[\text{Ni}(\text{dmit})_2]^-$ anions is one of our targets to engineer new physical properties, for example, phase transition and/or switching system in the solid state as a direct consequence of the molecular motion. However, until now, it should be noted that the intermolecular interactions between the supramolecular rotators and $[\text{Ni}(\text{dmit})_2]^-$ anions were too weak; therefore, we are adopting here a more direct approach to utilize the Keggin ion as a counter part.⁷ This is because the $[\text{PMo}_{12}\text{O}_{40}]$ Keggin cluster has basic outer oxygen atoms presented in 3D, which should be able to form stronger intermolecular interactions with the supramolecular cations. As such, these interactions could enhance the magnitude of the coupling between the magnetic units and the rotating units within the crystalline array. Furthermore, the nanoscale POM Keggin is a very useful building block to construct 3D arrays of the supramolecular cation system. By achieving the expansion of the 3D array compared to the structure of the $[\text{Ni}(\text{dmit})_2]$, the resulting lattice should be able to have enough void space to incorporate a building block that can act as a rotator.^{7,8}

Crystals of $(\text{Cs}^+)_3([\text{18}]\text{crown-6})_3(\text{H}^+)_2[\text{PMo}_{12}\text{O}_{40}](\text{CH}_3\text{CN})$ (**1**) were formed by a diffusion process between $\text{CsI}/[\text{18}]\text{crown-6}$ and $\text{H}^+[\text{PMo}_{12}\text{O}_{40}]\cdot 20\text{H}_2\text{O}$ in CH_3CN , yielding single crystals as black plates.¹¹ The direct reaction between $(\text{H}^+)_3[\text{PMo}_{12}\text{O}_{40}]^{3-}$ and CsI in CH_3CN yielded a black-colored powder $(\text{Cs}^+)_x[\text{PMo}_{12}\text{O}_{40}]$ salt, whereas the presence of [18]crown-6 in CH_3CN provided high-quality single crystals

* Corresponding Authors. Phone: +81-11-706-2884. Fax: +81-11-706-4972. E-mail: takuta@es.hokudai.ac.jp (T. A.) and tnaka@es.hokudai.ac.jp (T. N.).

[†] Research Institute for Electronic Science, Hokkaido University.

[‡] Graduate School of Environmental Earth Science, Hokkaido University.

[§] CREST.

[△] Graduate School of Science, Hokkaido University.

[⊥] University of Glasgow.

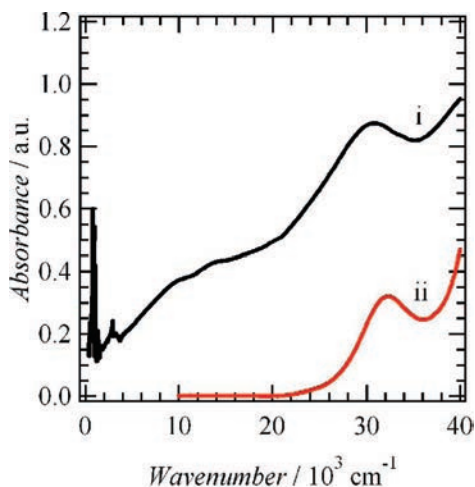


Figure 1. Electronic spectra of (i) salt **1** in KBr pellet (black) and (ii) $(\text{H}^+)_3[\text{PMo}_{12}\text{O}_{40}]^{3-}$ in DMF (red). The electron-reduced $[\text{PMo}_{12}\text{O}_{40}]^{5-}$ state was confirmed by the existence of electronic absorption at NIR and IR energy regions.

of salt **1**. Importantly, the incorporation of [18]crown-6 was effective in increasing the crystalline properties of the electron-reduced $[\text{PMo}_{12}\text{O}_{40}]$ cluster. Although the initial $[\text{PMo}_{12}\text{O}_{40}]^{3-}$ is diamagnetic with hexavalent Mo^{VI} ions within the cluster, the $[\text{PMo}_{12}\text{O}_{40}]^{3-}$ is easily reduced to $[\text{PMo}_{12}\text{O}_{40}]^{4-}$ with a total $S = 1/2$ spin and $[\text{PMo}_{12}\text{O}_{40}]^{5-}$ with two $S = 1/2$ spins within the cluster. Thus, the crystallization process with an excess of iodide causes an electron-transfer process from I^- ($3\text{I}^- = \text{I}_3^- + 2\text{e}^-$) to $[\text{PMo}_{12}\text{O}_{40}]^{3-}$ and the reduction of the material, resulting in the crystals changing color from bright-yellow to black. Figure 1 shows the electronic spectra of salt **1** in KBr pellet and $(\text{H}^+)_3[\text{PMo}_{12}\text{O}_{40}]^{3-}$ in DMF. The electronic spectrum of $[\text{PMo}_{12}\text{O}_{40}]^{3-}$ showed a broad absorption maximum at $32.0 \times 10^3 \text{ cm}^{-1}$, whereas salt **1** indicated electronic transitions at 9.8 , 13.9 , and $30.3 \times 10^3 \text{ cm}^{-1}$. The yellow-colored $(\text{H}^+)_3[\text{PMo}_{12}\text{O}_{40}]^{3-}$ did not show the d–d transition (spectrum (ii) in Figure 1) because of the $(4d)^0$ electronic structure of the Mo^{VI} ions. The electronic absorption at $32.0 \times 10^3 \text{ cm}^{-1}$ has been assigned to the metal–ligand charge-transfer electronic excitation from the doubly occupied oxo-orbitals to the unoccupied d-orbitals of Mo^{VI} .¹² On the other hand, the electronic spectra of salt **1** showed a broad absorption in the vis–NIR–IR energy region. Because the octahedral coordination of six oxygen atoms to Mo^{V} gives a crystal field splitting, the energy separation of which was usually larger than $10 \times 10^3 \text{ cm}^{-1}$, the low energy electronic absorption in salt **1** at $9.8 \times 10^3 \text{ cm}^{-1}$ was assigned to the intervalence transition from Mo^{V} to Mo^{VI} .^{10,12} The absorption band at $13.9 \times 10^3 \text{ cm}^{-1}$ was observed in the typical energy region of the d–d transitions of Mo^{V} ion.

The temperature-dependent molar magnetic susceptibility (T vs χ_{mol}) of salt **1** showed a small $\chi_{\text{mol}}T$ value of $0.01 \text{ emu} \cdot \text{K} \cdot \text{mol}^{-1}$ ($2 < T < 300 \text{ K}$), which is lower than expected for the one-electron-reduced Keggin; therefore, it was concluded that the electronic structure of $[\text{PMo}_{12}\text{O}_{40}]$ in salt **1** was best described as originating from the two-electron-reduced $[\text{PMo}_{12}\text{O}_{40}]^{5-}$, where two $S = 1/2$ spins are antiferromagnetically coupled to each other. From the elemental analysis, X-ray crystal structural analysis, optical spectra, and magnetic susceptibility, the stoichiometry of salt **1** was deduced to be $(\text{Cs}^+)_3([\text{18}]\text{crown-6})_3(\text{H}^+)_2[\text{PMo}_{12}\text{O}_{40}]^{5-}(\text{CH}_3\text{CN})$, where two protons are required to compensate the charge of the $[\text{PMo}_{12}\text{O}_{40}]^{5-}$ anion. Although the exact positions of the two

protons in the structure are unclear, several potential sites that could bind these protons are observed.

The examination of the structure of **1** shows that half a unit of $[\text{PMo}_{12}\text{O}_{40}]$ and two [18]crown-6 molecules (**A** and **B**) are incorporated in the asymmetric unit ($T = 163 \text{ K}$).¹⁴ Two kinds of orientational disorder present in the [18]crown-6 **A** were confirmed at 163 K, where the first [18]crown-6 was rotated 30° to the second one (Figure 2a,b). An average structure of the two orientations was observed in the crystal structural analysis. The same type of orientational disorder has been observed in the crystal structure of $\text{Cs}^+([\text{18}]\text{crown-6})_3[\text{Ni}(\text{dmit})_2]_2$ at temperatures above 250 K.^{7a} To confirm the temperature-dependent orientational changes in [18]crown-6 **A**, the crystal structure of salt **1** was evaluated at 100 K. Although the positional disorder associated with the [18]crown-6 **B** was observed at 100 K, the two orientations merge to one [18]crown-6 **A** orientation (lower-figure in Figure 2b). The molecular rotation of [18]crown-6 **A** was frozen at 100 K. Although it was difficult to determine the precise atomic positions because of the significant disorder in [18]crown-6 **B**, the Cs^+ ion could be clearly located, interacting with the six oxygen atoms of [18]crown-6 **B** and one nitrogen atom of CH_3CN , coordinated as an axial ligand. Four kinds of positional disorder were confirmed in [18]crown-6 **B** (Figure 2c), where one of the four disordered arrangements was introduced into the crystal. The $(\text{Cs}^+)_2([\text{18}]\text{crown-6 A})_2[\text{PMo}_{12}\text{O}_{40}]^{5-}$ is fundamental to the structural unit in salt **1**, where two $(\text{Cs}^+)([\text{18}]\text{crown-6 A})$ supramolecular cations are interacting with one $[\text{PMo}_{12}\text{O}_{40}]^{5-}$ at the upper and lower positions of the Keggin terminal oxo framework, as shown in Figure 2a. Because the diameter of the [18]crown-6 molecule ($\sim 1 \text{ nm}$) is complementary with that of the $[\text{PMo}_{12}\text{O}_{40}]$ cluster, a cylindrical $(\text{Cs}^+)_2([\text{18}]\text{crown-6})_2[\text{PMo}_{12}\text{O}_{40}]^{5-}$ with a diameter of $\sim 1 \text{ nm}$ and a height of $\sim 1.6 \text{ nm}$ was observed (Figure 2a). A typical $(\text{Cs}^+)([\text{18}]\text{crown-6 A})$ structure with six Cs^+ –O interatomic interactions with an average distance of 3.28 \AA was observed, whereas four bridging oxygen atoms at the Mo –O– Mo bonds of $[\text{PMo}_{12}\text{O}_{40}]$ interacted with the Cs^+ ion with an average Cs^+ –O distance of 3.36 \AA .¹⁵ The sum of the ionic radius of Cs^+ with a coordination number of 10 (1.81 \AA) and the van der Waals radius of oxygen (1.52 \AA) is similar to the average Cs^+ –O distances found in salt **1**. Therefore, the Cs^+ ion was moderately coordinated by 10 oxygen atoms of [18]crown-6 and $[\text{PMo}_{12}\text{O}_{40}]^{5-}$, forming a cylindrical $(\text{Cs}^+)_2([\text{18}]\text{crown-6})_2[\text{PMo}_{12}\text{O}_{40}]^{5-}$ molecular assembly. The oxygen atoms of $[\text{PMo}_{12}\text{O}_{40}]^{5-}$ interact directly with the molecular rotators of [18]crown-6 through the Cs^+ cation.

Panels d and e of Figure 2 show the unit cell of salt **1** viewed along the c -axis and the b -axis, respectively. The cylindrical $(\text{Cs}^+)_2([\text{18}]\text{crown-6})_2[\text{PMo}_{12}\text{O}_{40}]^{5-}$ units were arranged within the ab -plane (Figure 2d), in which four $(\text{Cs}^+)([\text{18}]\text{crown-6 A})$ units were orthogonally assembled together to form the tetramer unit. Each $[\text{PMo}_{12}\text{O}_{40}]^{5-}$ cluster connected by the tetramers formed a 2D layer structure, and each layer was stacked along the c -axis. The space shown in the ac -plane in Figure 2e is occupied by the $(\text{Cs}^+)([\text{18}]\text{crown-6 B})(\text{CH}_3\text{CN})$ units.

The temperature-dependent ^1H NMR spectra of salt **1** were measured to evaluate the dynamic properties of the [18]crown-6 molecules in the temperature range from 120 to 340 K.¹⁶ The thermal stability of salt **1** was evaluated by thermogravimetry differential thermal analysis (TG-DTA) with a scanning rate of $5 \text{ K} \cdot \text{min}^{-1}$ under N_2 flow (Figure S5). Because a gradual weight loss was observed above 300 K, the elimination of the solvent molecules of CH_3CN occurred at room temperature. The

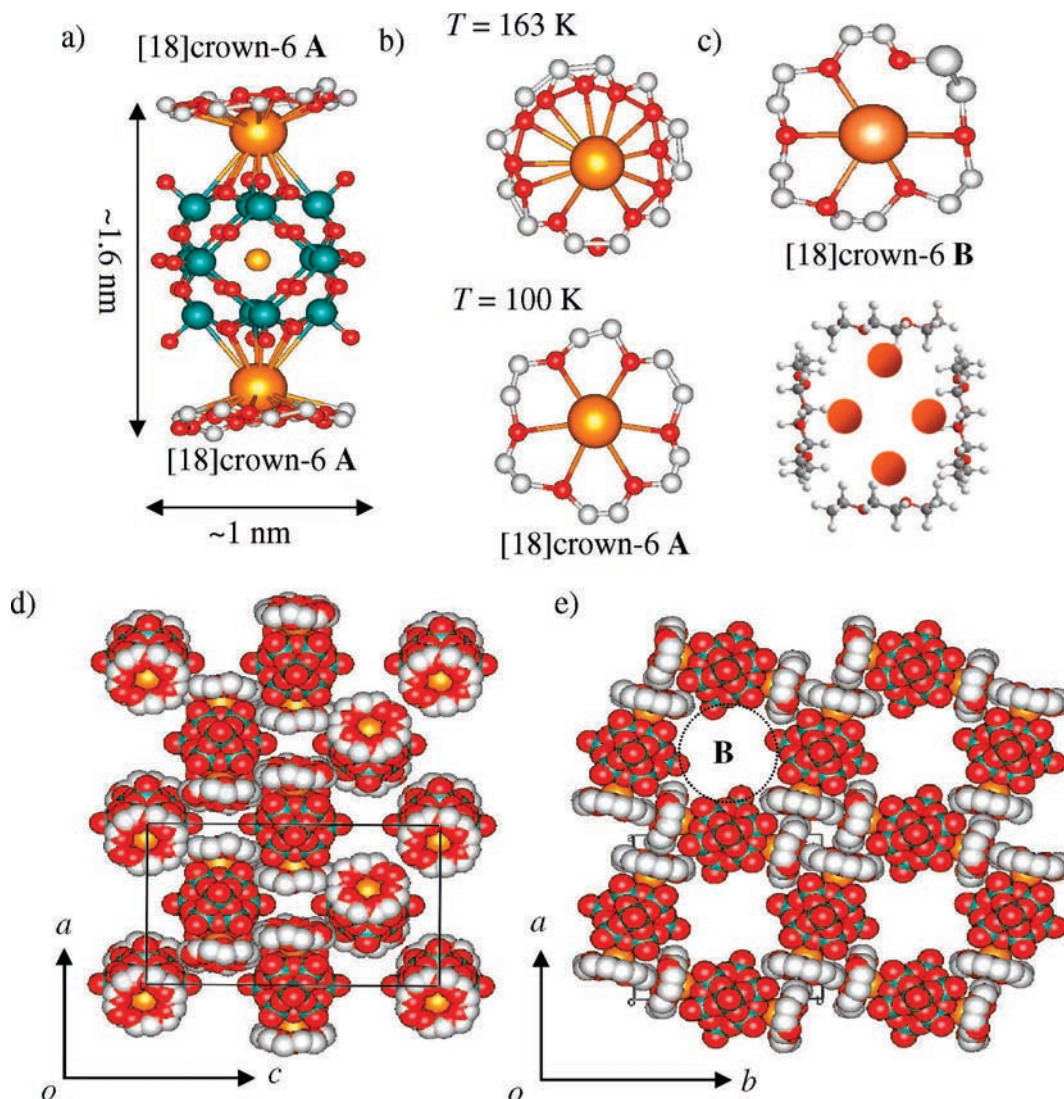


Figure 2. Crystal structure of salt **1**. (a) Basic $(\text{Cs}^+)_2([\text{18}]\text{crown-6 A})_2[\text{PMo}_{12}\text{O}_{40}]^{5-}$ structure; the height and diameter of the unit are 1.6 and 1.0 nm, respectively. (b) Orientation disorder structure of $[\text{18}]\text{crown-6 A}$ at $T = 163$ K (upper figure) and freeze structure of $[\text{18}]\text{crown-6 A}$ at $T = 100$ K (lower figure). Two kinds of orientations with a rotation angle of 30° were overlapped at 163 K, whereas one kind of orientation was confirmed by the structural analysis at 100 K. (c) Selected orientation of $[\text{18}]\text{crown-6 B}$ (top) and schematic representation of four positional disordered arrangements (bottom). One of the four disordered arrangements of $[\text{18}]\text{crown-6 B}$ and one CH_3CN were introduced into the crystalline space of **B** in panel e. (d) Unit cell viewed along the c -axis. (e) Unit cell viewed along the b -axis. $(\text{Cs}^+)([\text{18}]\text{crown-6 B})(\text{CH}_3\text{CN})$ units were omitted in the figure.

magnitude of the weight loss ($\sim 1\%$) at 340 K was slightly less than the calculated weight loss of one CH_3CN from $\text{C}_{38}\text{H}_{75}\text{NO}_{58}\text{PMo}_{12}\text{Cs}_3$ ($\sim 1.3\%$). The XRD profiles of salt **1** at 320 K were consistent with those at 300 K (Figure S6), suggesting that the structure of the crystal lattice remains unchanged in the absence of CH_3CN solvent at 320 K. Because the low thermal stability of salt **1** was confirmed by the TG-DTA diagram, the ^1H NMR measurements were started at 120 K with freshly prepared salt **1**.

The ^1H NMR spectra of salt **1** are clearly composed of two kinds of signals (Figure 3a and Figure S7). The differential spectra (red lines) were evaluated in order to extract the information on the narrow signal assigned to $[\text{18}]\text{crown-6 B}$. The full width at half-maximum (ΔH_A) and peak-to-peak line width (ΔH_B) of the differential spectra correspond to $[\text{18}]\text{crown-6 A}$ and $[\text{18}]\text{crown-6 B}$, respectively (Figure 3b). Because the protons of $[\text{18}]\text{crown-6 A}$ ($24\text{H} \times 2$), $[\text{18}]\text{crown-6 B}$ (24H), one CH_3CN (3H), and two H^+ of salt **1** are detected in the NMR experiment, the spectrum is largely dominated by the two

components of $[\text{18}]\text{crown-6 A}$ (48H) and $[\text{18}]\text{crown-6 B}$ (24H). The crystallographically equivalent two $[\text{18}]\text{crown-6 A}$ molecules in the cylindrical $(\text{Cs}^+)_2([\text{18}]\text{crown-6 A})_2[\text{PMo}_{12}\text{O}_{40}]^{5-}$ should have the same T vs ΔH behavior, whereas the $(\text{Cs}^+)([\text{18}]\text{crown-6 B})$ unit can show a different T vs ΔH behavior from those in $[\text{18}]\text{crown-6 A}$. From the X-ray crystal structural analysis, the atomic arrangement of the $[\text{18}]\text{crown-6 B}$ is much more disordered than that of $[\text{18}]\text{crown-6 A}$. Therefore, the ΔH_B corresponds to $[\text{18}]\text{crown-6 B}$.

When the temperature was lowered down to 120 K, a broadening of ΔH was observed around 220 K (Figure 3b). The ΔH values at temperatures below 200 K were almost constant at ~ 50 kHz, and those above 300 K also reached a constant value of ~ 10 kHz. The magnitudes of ΔH in the rotational and frozen states for $[\text{18}]\text{crown-6}$ have been reported at ~ 60 and ~ 10 kHz, and the dynamic disorder without the rotation of $[\text{18}]\text{crown-6}$ yielded a ΔH value of 20–30 kHz.^{3b,7a,b} Therefore, the thermal energy of $k_B T$ (~ 220 K) activates the rotation of $[\text{18}]\text{crown-6}$ in salt **1** with a rotary frequency of several tens of

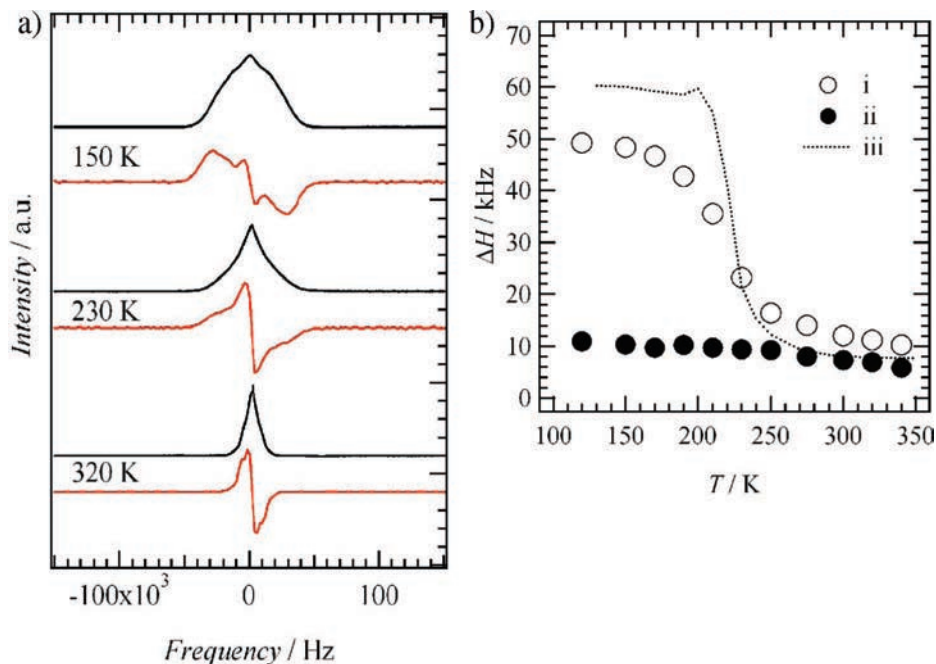


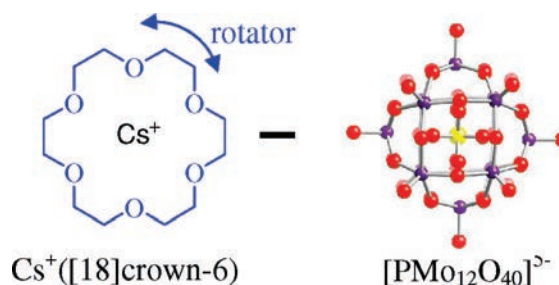
Figure 3. Solid-state ^1H NMR spectra of salt **1**. (a) Temperature-dependent spectra (upper black line) and differential spectra (lower red line) at 150, 230, and 320 K. (b) Temperature dependence of the line width of [18]crown-6 **A** (open circle: ΔH_A), the line width of [18]crown-6 **B** (filled circle: ΔH_B), and ΔH of the reference salt of $(\text{Cs}^+)_2[\text{18crown-6}]_3[\text{Ni}(\text{dmit})_2]_2^-$ (dashed line).

kHz. At about 40 kHz, the change of the ΔH_A values, which occurred when the temperature was lowered, was almost the same as that of the molecular rotation of [18]crown-6 in $(\text{Cs}^+)_2[\text{18crown-6}]_3[\text{Ni}(\text{dmit})_2]_2^-$ salt (**2**).^{7a} The similar type of orientational disorder of [18]crown-6 for salts **1** and **2** revealed a temperature-dependent line width. The crossover temperatures from the rotation state ($T > 220$ K) to the frozen state ($T < 220$ K) of salts **1** and **2** were consistent with each other. Although the interaction between $[\text{PMo}_{12}\text{O}_{40}]^{5-}$ and [18]crown-6 **A** occurred through the Cs^+-O interactions in salt **1**, the thermally activated molecular motion of orientationally disordered [18]crown-6 showed the same activation behavior. On the other hand, a temperature-independent narrow line width was observed at a ΔH_B of ~ 10 kHz in the entire temperature range, suggesting that the molecular rotation of [18]crown-6 **B** occurred even at 120 K.

In the *ac*-plane, the molecular planes of the four [18]crown-6 molecules (tetramer) are arranged perpendicularly to each other (Figure 2b). Although each [18]crown-6 molecule in the tetramer can show a collective rotation of the [18]crown-6, significant evidence of a phase transition in salt **1** was not detected at ~ 200 K from the temperature-dependent DSC measurements. Therefore, the molecular rotation of [18]crown-6 is a thermally activated random motion. However, a slight enhancement of the dielectric constant was observed at temperatures above 200 K (Figure S8). Because the dielectric constant is not affected by the symmetric [18]crown-6 molecules, the thermally activated molecular fluctuation of [18]crown-6 is expected to influence the dielectric response of the crystal indirectly.

In conclusion, the thermally activated rotator of [18]crown-6 was complexed with the surface of a two-electron-reduced $[\text{PMo}_{12}\text{O}_{40}]^{5-}$ cluster through Cs^+-O interactions. The molecular rotations of [18]crown-6 were confirmed in the temperature-dependent ^1H NMR spectra, which revealed two kinds of rotational frequencies. A cylindrical molecular assembly of $(\text{Cs}^+)_2[\text{18crown-6}]_2[\text{PMo}_{12}\text{O}_{40}]^{5-}$ was constructed by Cs^+-O

Scheme 1. Schematic of the Molecular Structures of $\text{Cs}^+[\text{18crown-6}]$ and $[\text{PMo}_{12}\text{O}_{40}]^{5-}$ in Salt **1. Red, violet, and yellow spheres of $[\text{PMo}_{12}\text{O}_{40}]^{5-}$ cluster are O, Mo, and P atoms, respectively. The $\text{Cs}^+[\text{18crown-6}]$ was introduced as the counteraction of $[\text{PMo}_{12}\text{O}_{40}]^{5-}$, where the [18]crown-6 molecules acted as the solid-state molecular rotators.**



interatomic interactions between Cs^+ and [18]crown-6 and/or $[\text{PMo}_{12}\text{O}_{40}]^{5-}$, which has the potential of increasing the coupling magnitude between the molecular rotators and magnetic spins. The 3D molecular structure of the α - $[\text{PMo}_{12}\text{O}_{40}]$ cluster was fitted to the diameter of the [18]crown-6 molecule, forming cylindrical rodlike supramolecules, where the molecular rotation of [18]crown-6 in the solid state was allowed.

Acknowledgment. This work was partly supported by a Grant-in-Aid for Science Research from the Ministry of Education, Culture, Sports, Science, and Technology of Japan.

Supporting Information Available: Temperature-dependent magnetic susceptibility, IR, temperature-dependent dielectric properties, XRD, solid-state ^1H NMR spectra, TG-DTA of salt **1**. Atomic numbering scheme of structural analysis of salt **1** at 163 and 100 K (CIF). These materials are available free of charge via the Internet at <http://pubs.acs.org>.

References

- (1) See for example (a) Balzani, V.; Credi, A.; Raymo, F.; Stoddart, J. F. *Angew. Chem., Int. Ed.* **2000**, *39*, 3348. (b) Kottas, G. S.; Clarke,

- L. I.; Hornek, D.; Michl, J. *Chem. Rev.* **2005**, *105*, 1281. (c) Kay, E. R.; Leigh, D. A.; Zerbetto, F. *Angew. Chem., Int. Ed.* **2007**, *46*, 72.
- (2) (a) Kelly, T. R.; Silva, H. D.; Silva, R. A. *Nature* **1999**, *401*, 150. (b) Koumura, N.; Zijlstra, R. W. J.; Delden, R. A.; Harada, N.; Feringa, B. L. *Nature* **1999**, *401*, 152. (c) Leigh, D. A.; Wong, J. Y.; Dehez, F.; Zerbetto, F. *Nature* **2003**, *424*, 174.
- (3) (a) Buchanan, G. W.; Kirby, R. A.; Ripmeester, J. A.; Ratcliffe, C. I. *Tetrahedron Lett.* **1987**, *28*, 4783. (b) Ratcliffe, C. I.; Ripmeester, J. A.; Buchanan, G. W.; Denike, J. M. *J. Am. Chem. Soc.* **1992**, *114*, 3294. (c) Bedard, T. C.; Moore, J. S. *J. Am. Chem. Soc.* **1995**, *117*, 10662.
- (4) (a) Dominguez, Z.; Dang, H.; Strouse, M. J.; Garcia-Garibay, M. A. *J. Am. Chem. Soc.* **2002**, *124*, 2398. (b) Godinez, C. E.; Zepeda, G.; Garcia-Garibay, M. A. *J. Am. Chem. Soc.* **2002**, *124*, 4701. (c) Dominguez, Z.; Dang, H.; Strouse, M. J.; Garcia-Garibay, M. A. *J. Am. Chem. Soc.* **2002**, *124*, 7719. (d) Dominguez, Z.; Khuong, T. V.; Dang, H.; Sanrame, C. N.; Nuñez, J. E.; Garcia-Garibay, M. A. *J. Am. Chem. Soc.* **2003**, *125*, 8827. (e) Dominguez, Z.; Khuong, T. A.; Dang, H.; Sanrame, C. N.; Nuñez, J. E.; Garcia-Garibay, M. A. *J. Am. Chem. Soc.* **2003**, *125*, 8827. (f) Karlen, S. D.; Ortiz, R.; Chapman, O. L.; Garcia-Garibay, M. A. *J. Am. Chem. Soc.* **2005**, *127*, 6554. (g) Karlen, S. D.; Garcia-Garibay, M. A. *Chem. Commun.* **2005**, 189. (h) Horansky, R. D.; Clarke, L. I.; Price, J. C.; Khuong, T. V.; Jarowski, P. D.; Garcia-Garibay, M. A. *Phys. Rev. B* **2005**, *72*, 014302. (i) Karlen, S. D.; Ortiz, R.; Chapman, O. L.; Garcia-Garibay, M. A. *J. Am. Chem. Soc.* **2005**, *127*, 6554. (j) Karlen, S. D.; Khan, I. S.; Garcia-Garibay, M. A. *Cryst. Growth Des.* **2005**, *5*, 53. (k) Horansky, R. D.; Clarke, L. I.; Winston, E. B.; Price, J. C.; Karlen, S. D.; Jarowski, P. D.; Santillan, R.; Garcia-Garibay, M. A. *Phys. Rev. B* **2006**, *74*, 054306. (l) Garcia-Garibay, M. A. *Proc. Natl. Acad. Sci. U.S.A.* **2005**, *102*, 10771. (m) Khuong, T. V.; Nuñez, J. E.; Dodinez, C. E.; Garcia-Garibay, M. A. *Acc. Chem. Res.* **2006**, *39*, 413. (n) Khuong, T. V.; Dang, H.; Jarowski, P. D.; Maverick, E. F.; Garcia-Garibay, M. A. *J. Am. Chem. Soc.* **2007**, *129*, 839.
- (5) (a) Clarke, L. I.; Horinek, D.; Kottas, G. S.; Varaksa, N.; Magnera, T. F.; Hinderer, T. P.; Horansky, R. D.; Michl, J.; Price, J. C. *Nanotechnology* **2002**, *13*, 533. (b) Xu, D.; Kelly, T. R.; Ganz, E. *Nanotechnology* **2003**, *14*, 566. (c) Gardinier, J. R.; Pellechia, P. J.; Smith, M. D. *J. Am. Chem. Soc.* **2005**, *127*, 12449. (d) Horike, S.; Matsuda, R.; Tanaka, D.; Matsubara, S.; Mizuno, M.; Endo, K.; Kitagawa, S. *Angew. Chem., Int. Ed.* **2006**, *45*, 7226.
- (6) (a) Nakamura, T.; Akutagawa, T.; Honda, K.; Underhill, A. E.; Coomber, A. T.; Friend, R. H. *Nature* **1998**, *394*, 159. (b) Akutagawa, T.; Hasegawa, T.; Nakamura, T.; Takeda, S.; Inabe, T.; Sugiura, K.; Sakata, T.; Underhill, A. E. *Chem. Eur. J.* **2001**, *7*, 4902. (c) Akutagawa, T.; Hasegawa, T.; Nakamura, T.; Inabe, T. *J. Am. Chem. Soc.* **2002**, *124*, 8903.
- (7) (a) Akutagawa, T.; Shitagami, K.; Nishihara, S.; Takeda, S.; Hasegawa, T.; Nakamura, T.; Hosokoshi, Y.; Inoue, K.; Ikeuchi, S.; Miyazaki, Y.; Saito, K. *J. Am. Chem. Soc.* **2005**, *127*, 4397. (b) Ikeuchi, S.; Miyazaki, Y.; Takeda, S.; Akutagawa, T.; Nishihara, S.; Nakamura, T.; Saito, K. *J. Chem. Phys.* **2005**, *123*, 044514. (c) Sato, D.; Akutagawa, T.; Takeda, S.; Noro, S.; Nakamura, T. *Inorg. Chem.* **2007**, *46*, 363. (d) Nishihara, S.; Akutagawa, T.; Sato, D.; Takeda, S.; Noro, S.; Nakamura, T. *Chem. Asian J.* **2007**, *2*, 1983.
- (8) (a) Akutagawa, T.; Endo, D.; Imai, H.; Noro, S.; Cronin, L.; Nakamura, T. *Inorg. Chem.* **2006**, *45*, 8626. (b) Akutagawa, T.; Endo, D.; Noro, S.; Cronin, L.; Nakamura, T. *Coord. Chem. Rev.* **2007**, *251*, 2547.
- (9) (a) Cronin, L. *Compr. Coord. Chem.* **2004**, *7*, 1. (b) Long, D. L.; Burkholder, E.; Cronin, L. *Chem. Soc. Rev.* **2007**, 105.
- (10) (a) Pope, M. T. *Heteropoly and Isopoly Oxometalates*; Springer-Verlag: Berlin, 1983; p 109. (b) Prados, R. A.; Pope, M. T. *Inorg. Chem.* **1976**, *15*, 2547. (c) Sanchez, C.; Livage, J.; Launary, J. P.; Fournier, M.; Jeannin, Y. *J. Am. Chem. Soc.* **1982**, *104*, 3194.
- (11) Single crystals of salt **1** were grown by a diffusion method between $(\text{H}^+)_3[\text{PMo}_{12}\text{O}_{40}] \cdot 20\text{H}_2\text{O}$ (130 mg) and CsI (380 mg)/[18]crown-6 (350 mg) in 50 mL anhydrous CH_3CN during two weeks. Elemental analysis for $\text{C}_{38}\text{H}_{75}\text{NO}_{58}\text{PMo}_{12}\text{Cs}_3$. Calcd: C, 14.94; H, 2.48; N, 0.46. Found: C, 14.58; H, 2.48; N, 0.87%.
- (12) (a) Prados, R. A.; Meiklejohn, P. T.; Pope, M. T. *J. Am. Chem. Soc.* **1974**, *96*, 1261. (b) Prados, R. A.; Pope, M. T. *Inorg. Chem.* **1976**, *15*, 2547. (c) Sanchez, C.; Livage, J.; Launary, J. P.; Fournier, M.; Jeannin, Y. *J. Am. Chem. Soc.* **1982**, *104*, 3194.
- (13) (a) Ouahab, L.; Bencharif, M.; Mhanni, A.; Pelloquin, D.; Halet, J.-F.; Peña, O.; Padiou, J.; Grandjean, D.; Garrigou-Lagrange, C.; Amiell, J.; Delhaes, P. *Chem. Mater.* **1992**, *4*, 666. (b) Gómez-García, C. J.; Ouahab, L.; Giménez-Saiz, C.; Triki, S.; Coronado, E.; Delhaes, P. *Angew. Chem., Int. Ed. Engl.* **1994**, *33*, 223. (c) Bellitto, C.; Bonamico, M.; Fares, V.; Federici, F.; Righini, G.; Kurmoo, M.; Day, P. *Chem. Mater.* **1995**, *7*, 1475. (d) Coronado, E.; Galan-Mascarós, J. R.; Giménez-Saiz, C.; Gómez-García, C. J.; Triki, S. *J. Am. Chem. Soc.* **1998**, *120*, 4671. (e) Coronado, E.; Galan-Mascarós, J. R.; Giménez-Saiz, C.; Gómez-García, C. J.; Falvello, L. R.; Delhaes, P. *Inorg. Chem.* **1998**, *37*, 2183.
- (14) Crystal structure analysis for $(\text{Cs}^+)_3[\text{18}]_{\text{crown-6}}[\text{PMo}_{12}\text{O}_{40}](\text{CH}_3\text{CN})_{\text{C}_{38}\text{H}_{75}\text{NO}_{58}\text{PMo}_{12}\text{Cs}_3}$. $T = 163$ K; tetragonal, space group $I4_2d$, $a = b = 21.823(12)$, $c = 34.6801(19)$ Å, $V = 16500.0(16)$ Å³, $D_c = 2.457$ g·cm⁻³, $Z = 8$. $T = 100$ K; tetragonal, space group $I4_2d$, $a = b = 21.92(4)$, $c = 34.55(7)$ Å, $V = 16609(6)$ Å³, $D_c = 2.441$ g·cm⁻³, $Z = 8$. Black platelike crystal (0.30 × 0.1 × 0.05 mm). Data were collected on a Rigaku Raxis-Rapid diffractometer using Mo $K\alpha$ ($\lambda = 0.71073$ Å) radiation from a graphite monochromator at 163 K. A total of 69597 reflections were collected; 9359 reflections are independent. Structure refinements were performed using the full-matrix least-squares method on F^2 . Calculations were performed using Crystal Structure software packages (Ver. 3.6, 2004, Rigaku Corporation and Molecular Structure Corporation) and SHELXL-97 software packages (Sheldrick, G. M. University of Göttingen, 1993/1997/2001). Parameters were refined using anisotropic temperature factors except for carbon atoms of [18]crown-6 and hydrogen atoms. $T = 163$ K: R_1 ($I > 2\sigma$) = 0.0599, $R(\text{all}) = 0.1010$, G.O.F. = 1.023, min and max residual electron densities of +0.62 and -0.77 e⁻/Å³. $T = 100$ K: R_1 ($I > 0.5\sigma$) = 0.0475, $R(\text{all}) = 0.0890$, G.O.F. = 1.066, min and max residual electron densities of +1.50 and -1.33 e⁻/Å³.
- (15) (a) Bondi, A. J. *Phys. Chem.* **1964**, *68*, 441. (b) *Handbook of Chemistry and Physics*, 83rd ed.; CRC Press: New York, 2002.
- (16) The solid-state wide-line ¹H NMR spectrum under the static condition of the sample was measured by a solid echo pulse sequence $\pi/2_x - \tau - \pi/2_y$, $\pi/2$ pulse width and τ were 1.2 μs and 10 μs , respectively. We used a Bruker DSX 300 spectrometer with an operating frequency of 300 MHz for proton.

CG060951+